CFD Final Project

Noah D. Brenowitz

May 20, 2013

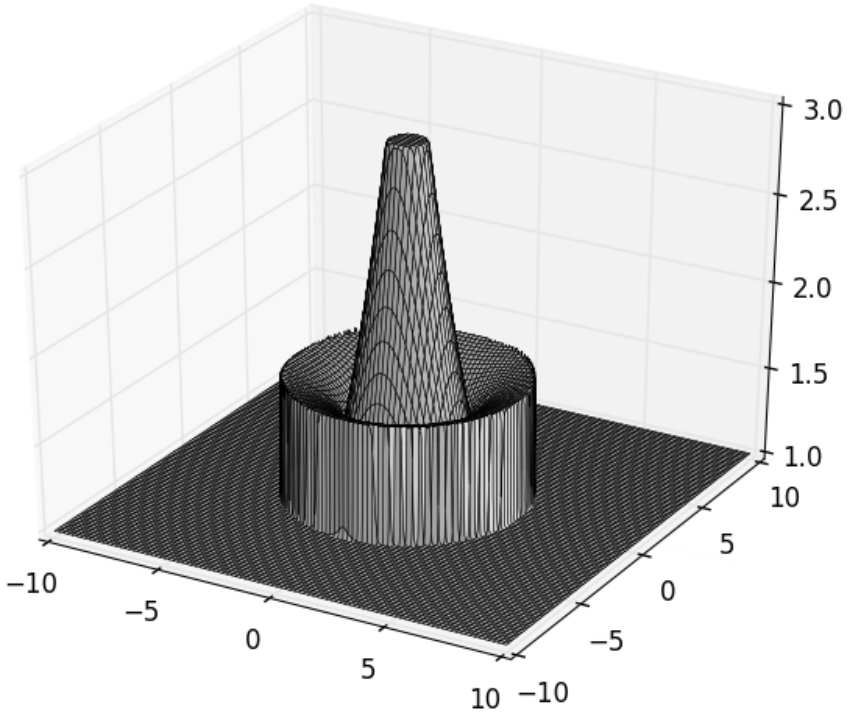

For this project, we implemented a high resolution Finite Volume Method (FVM) to solve the Shallow Water Equations (SWE) in both one and two dimensions:

$$\begin{pmatrix} h \\ hu \\ hv \end{pmatrix}_t + \begin{pmatrix} hu \\ \frac{1}{2}gh^2 + hu^2 \\ huv \end{pmatrix}_x + \begin{pmatrix} hv \\ huv \\ \frac{1}{2}gh^2 + hv^2 \end{pmatrix}_y = 0$$

These equations are a simplification for the full equations of motion under the assumption of constant density and hydrostatic balance. For convenience, we assume a flat-bottom scenario. An example of a shallow water flow is a Tsunami, which has long horizontal extent compared to the depth of the ocean. We also consider the Rotating SWE on an f-plane:

$$\begin{pmatrix} h \\ hu \\ hv \end{pmatrix}_t + \begin{pmatrix} hu \\ \frac{1}{2}gh^2 + hu^2 \\ huv \end{pmatrix}_x + \begin{pmatrix} hv \\ huv \\ \frac{1}{2}gh^2 + hv^2 \end{pmatrix}_y = -f \begin{pmatrix} 0 \\ -hv \\ hu \end{pmatrix}$$

which are a simplication of the equations of motion in a rotating plane. These equations are of great importance in Geophysical Fluid Dynamics (GFD), and the source terms on the right our known as the *coriolis* terms. In the nonconservation form, the balance $f \times u = -g\nabla h$ is know as *geostrophic* balance. For more information on these equation in the context of the atmosphere and ocean see [4].

The SWE cast in the above form are an example of a hyperbolic conservation law, so the methods implemented here are generally applicable. Other examples of hyperbolic systems are the equations for gas dynamics and Burger's equation.

1 Methods

The numerical schemes in this report were devoped in the textbook by Randal L. Leveque[2]. For the sake of brevity, I brush over details that are well explained in the text. The code is available on GitHub at `https://github.com/nbren12/cfd-final`. I have also provided a tar file along with this report, but I recommend GitHub, since you can look at my commits and browse the code easily. In the root of the code there is a `README.md`. Once again, this can be viewed easily at the link above.

1D Solver For the 1D solver, we implemented a Roe Averaging approximate Riemann solver. The precise form of the Roe Averaging fluxes is given in the Appendix of this report. To ensure this approximate solver produced entropy-condition satisfying solutions, we employed the *Harten-Hyman* entropy fix. To achieve high resolution, we used a fully discrete framework and modified the flux to achieve second order accuracy. This flux was then limited using a "Superbee" or a "minmod" (e.g. minimum modulus) limiter.

2D Solver The 2D solver with high resolution was implemented similarly to the 1D case. Roe averaging was used to solve the approximate riemann problem on each interface, and superbee-limited second order correction fluxes were applied. The main difference here, was that a roe solver in the y-direction was different, yet quite similar to the roe solver for the x-direction.

The real difference between the 1D and 2D cases arises in the application of corner-corrective fluxes at each interface to allow for proper upwinding and stability. At vertical interfaces (e.g. the left and right) the y-direction riemann solver is applied first-order x-direction fluctuations. The end result is a division of the right/left going fluctuations into right-then-up, right-then-down, left-then-up, and left-then-down fluctations. The right-then-up fluctuations are then used to modify

the fluxes in the horizontal interface to upper-right of the current interface, and analogously for the other corrections.

The same procedure is applied to the horizontal interfaces (e.g. up and down) to obtain modifying fluxes that go down-then-left, down-then right, etc. For more details, see Chapter 21 in [2].

Initial Conditions When considering a nonsmooth initial condition in 2D, it can important to implement the initial condition as an *average* over cells. This has the effect of smoothing the initial condition on coarse grids. To implement this, we first calculate the initial condition over an extremely fine grid (at least 7 times the resultion in each direction). Then, we interpolate this grid using "scipy.interpolate.RectBivariateSpline". This interpolant was then integrated over each coarse grid cell to obtain the averaged initial condition.

Boundary Conditions In this project we impemented three different types of boundary conditions in various combinations: periodic, outflow, and Neumann conditions. All the boundary conditions were implemented using ghost cells. For the high resolution method, two ghost cells in each direction were required. Periodic conditions were the simplest to implement $q_j = q_{j\%n}$ where $j\%n$ means j modulo n. Outflow conditions, which are the simplest of the "nonreflecting" boundary conditions, are achieved by zeroth order extrapolation: $q_{j \in ghost} = q_n$ or q_1 depending on whether the $j > n$ or $j < 1$. Neumann conditions were similarly implemented by an even extension across the interface: $q_{n+j} = q_{n-j}$ or $q_{1-j} = q_{1+j}$.

Source Terms Source term $q_t + \nabla \cdot f(q) = \psi(q)$ were handled using *Godunov* splitting, which is a fractional step method. First, the conservation law $q_t + \nabla \cdot f(q) = 0$ is advanced Δt using the schemes discussed above. Then, using this intermediate value as an initial condition, the ordinary differential equation $q_t = \psi(q)$ is advanced Δt. To solve integrate the ODE, I chose to use the simplest second-order Runge-Kutta method: the explicit midpoint rule:

$$\begin{aligned} q^* &= q^n + \frac{\Delta t}{2}\psi(q^n) \\ q^{n+1} &= q^n + \frac{\Delta t}{2}\psi(q^*) \end{aligned}$$

This approach was used for both the coriolis terms in the rotating shallow water equations, as well as the metric (e.g. r^{-1}) terms in the radial dam break problem.

Time Step For the following examples, we choose the time step to satisfy a CFL condition. For the shallow water system, the fastest riemann invariant travels at $\lambda = u + c$ or $u - c$. $c = \sqrt{gH}$. Assuming the velocity is less than the speed of gravity waves c, we can assume that $\lambda_{max} \approx c$. Therefore the CFL condition requires that

$$\lambda_{max}\frac{\Delta t}{\Delta x} \leq C.$$

In practice, we choose $\Delta t = \frac{\Delta x}{3c}$ to ensure stability.

2 Results

2.1 Dam Break

In this section, we aim to solve the dam break problem. This is simply the inital value problem

$$h(x,0) = \begin{cases} H+\eta & x<0 \\ H-\eta & x>0 \end{cases}$$

with the velocity at rest initially. For our purposes, we considered the situation $H = 2$ and $\eta = 1$, this is a large deviation compared to the overall depth, so one would expect high velocities. Gravity is taken to be 9.812. In particular, the Froude number for this system will be large. Numerically, we must solve on a finite grid, so we employed "outflow" extrapolation conditions described above. However, since the problem is hyperbolic, boundary condition information propogates at finite speed, and has no affect on some interior region of the solution. In particular, we solve this on the domain (-10,10). For simplicity of programming, we used the 2D solving code with an Nx2 grid, turned off the corner-correction fluxes, and used periodic boundary conditions on the vertical boundaries to ensure the solution matched the 1D solution.

The SWE with these intial conditions were solved using the methods outlined above, and Figure 1a contains a plot of the evolution of this solution. The solution at all times consists only of rarefaction waves and shocks. Therefore, the solution is piecewise linear with discontinouities. The to this particular Riemann problem is analytically known, but requires a nonlinear root solve, and it is easier to just use a very high resolution to obtain the "exact" evolution.

Figure 1: Time Evolution

(a) Dam Break (b) Radial Dam Break

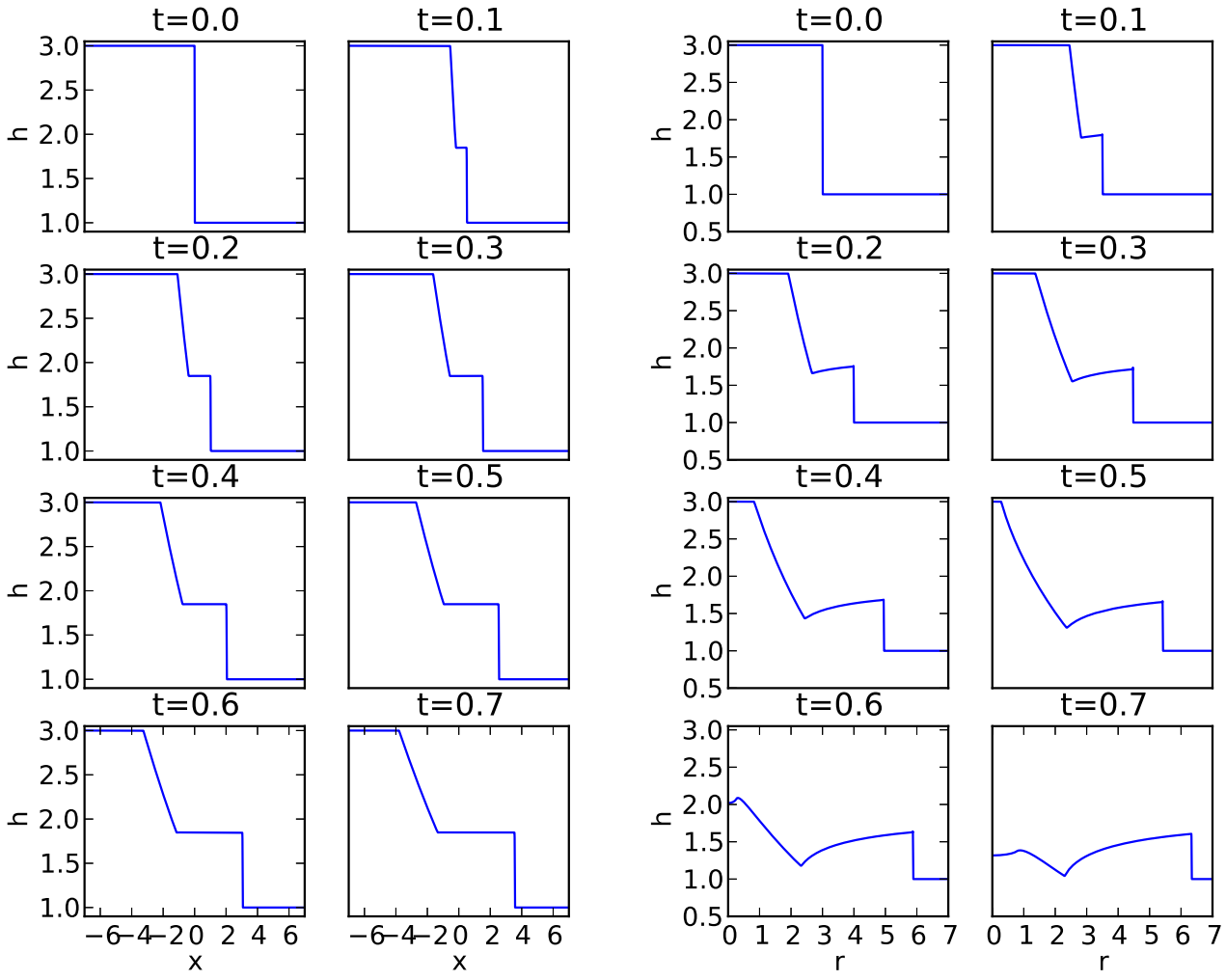

To analyze the performance of the various schemes and flux-limiters, we plot the numerical solutions at $t = .7$ in 1b. As expected, the HR schemes more accurately capture the sharp cornes of the rarefaction waves and shocks than the first-order Godunov scheme. Also, the "SuperBee" limiter appears to perform better than the "MinMod" limiter.

2.2 Radial Dam Break

To test the performance of the 2D HR solver, we use a radial dam break initial value problem:

$$h(x,0) = \begin{cases} H+\eta & |x| < R \\ H-\eta & |x| > R \end{cases}$$

Figure 2: Dam Break Scheme Comparison at $t = .7$

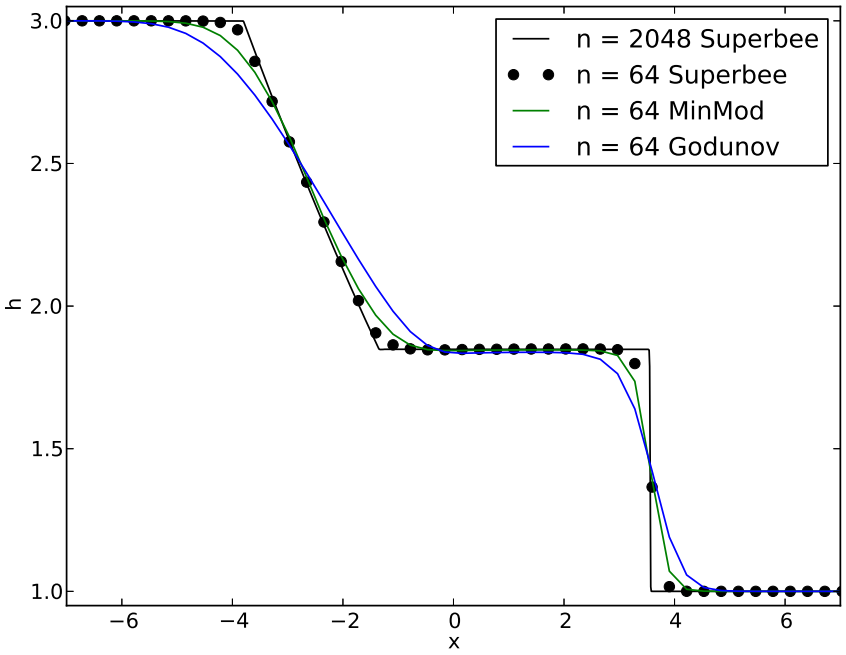

We solved this problem using the 2D solver on a square grid at various resolutions (on the domain $(-10, 10)^2$), the surface plot on the cover of this report is the height field at $t = .4$. As before, gravity is taken to be 9.812. The advantage of using this radially symmetric problem, was that we can also solving using the 1D solver! By casting the SWE in polar coordinates and assuming radial symmetry we obtain the following problem:

$$\begin{pmatrix} h \\ hu \end{pmatrix}_t + \begin{pmatrix} hu \\ hu^2 + \frac{1}{2}gh^2 \end{pmatrix}_x = -\frac{1}{r}\begin{pmatrix} hu \\ hu^2 \end{pmatrix}$$

where u is now the radial component of the velocity. The source term on the right is treated using the fractional step approach above. We can solve this 1D problem at extremely high resolution, so we in practice treat it as the exact solution. The evolution of the height field solved with $n = 4000$ is shown in Figure 1b. As before, the solution consists of shocks and rarefactions, but the source term, which dampens small r heavily, has added some smooth structure to the solution.

We first compare the 2D HR with superbee limiter and 2D Godunov methods, by making scatter plots between radius and height. These can be seen in Figure 3 . It is easy to see that that HR scheme does a much better job of approximating the "exact" solution than does the first order scheme.

A convergence analysis is shown Figure 4. We compare the HR scheme with and without corner flux correction, and without the entropy fix to the Godunov scheme with corner correction. Amongst the HR scheme there is little difference, but the error is lowest at most resolutions for the HR with corner correction and entropy fix. Notably, the HR schemes are all much better than the first order scheme; however, the *rate* of convergence is sublinear for all the schemes. . While it would be nice to see quadratic convergence for the HR schemes, it should not be expected because the solution is

Figure 3: Radial Dam Break Scheme Comparison at $t = .3$

(a) 100x100 High Resolution 2D vs 1D

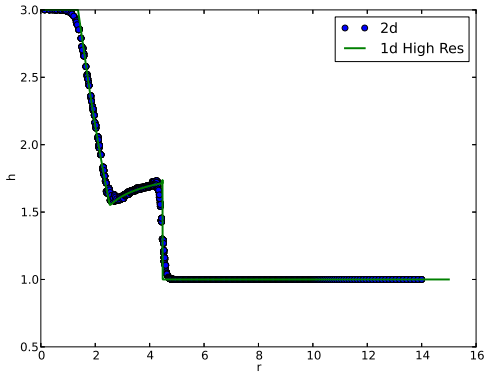

(b) 100x100 Godunov w/ Corner Fix 2D vs 1D

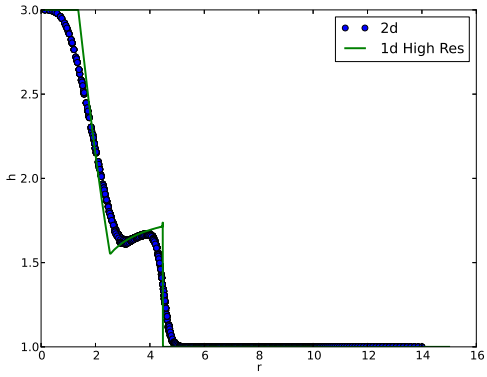

Figure 4: Radial Dam Break Convergence at $t = .7$

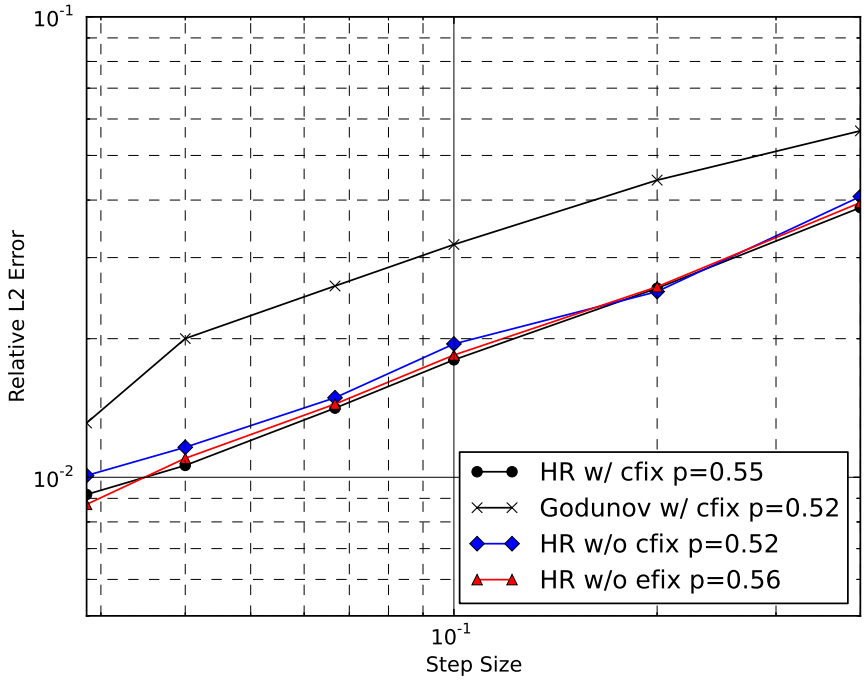

Figure 5: Corner fix performance at $t = .2$

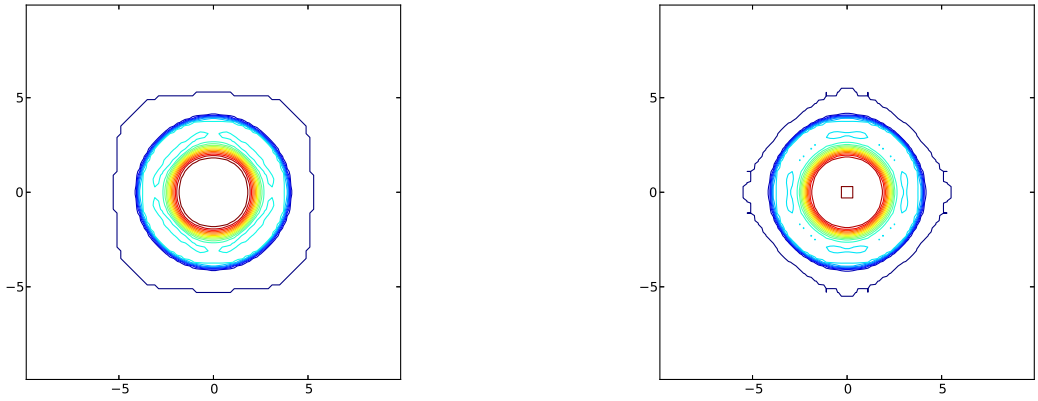

(a) Corner Fix

(b) No Corner Fix

obviously not smooth, and we considered global error estimates. Had we constrained this analysis to only smooth regions, the story could well be different.

Figure 4 did not show that corner flux correction significantly improves the error characterstics of the numerical solution. This could have happened because numerical diffusion blurred the solutions by $t = .7$ thereby removing the distortions in the non corner corrected solution. To explore this in further depth, we plot the two solutions with $n = 100$ at a shorter time ($t = .2$) in Figure 5. Qualititatively, the contours for the corner corrected solution is cleaner and shows less distortion and "boxiness" than the uncorrected version.

2.3 Geostrophic Adjustment

Now, we consider the Rotating SWE, and the geostrophic adjustment problem. This is an important problem in Geophysical Fluid Dynamics, because it explains how the dominant balance in atmosphere and ocean arises. The initial conditions are a dam break with mean height $H = 10$ and deviation $\eta = .1$. Gravity is taken to be .1, so that the gravity wave speed $c = \sqrt{gH} = 1$. We consider, a strongly rotating case with $f = 5$, and solve over the domain $(-1, 1)$. The coriolis source terms are treated using the fractional step procedure described above. The evolution is shown in Figure 7a and a comparison between HR and first order is shown in Figure 7b. As before, the HR scheme captures the sharp features much better.

Finally, a succesive errors convergence analysis comparing the 1D HR scheme is shown in Table 1. Because there is a very nonlinear smooth region in the solution, the HR scheme is able to show faster *global* convergence than the first order scheme. In fact, the convergence is nearly twice as large for the HR scheme.

3 Conclusion

In this report, we implemented a "High Resolution" method for solving the Shallow Water Equations in both rotating and non-rotating settings. The numerical schemes were given in the text by Leveque [2]. On the test problems considered, the HR scheme, which has analytical second order accuracy, was not able to achieve quadratic error reduction. This is expected given the non-smooth nature of

Figure 6: Geostrophic Adjustment

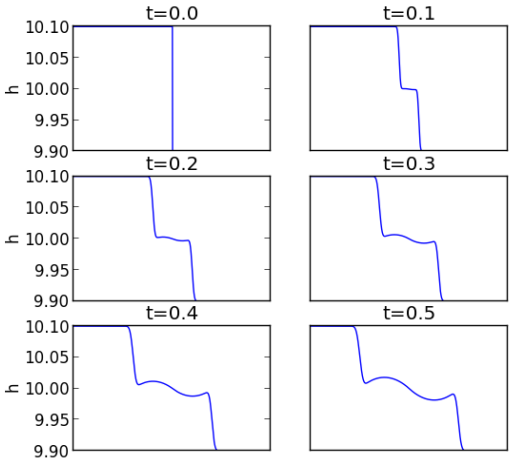

(a) Time Evolution

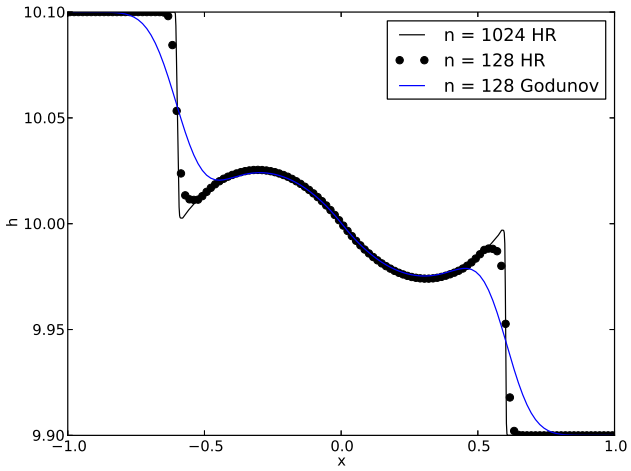

(b) Scheme Comparison at $t = .6$

Table 1: Geostrophic Adjustment Convergence

(a) High Resolution

n	$\|u_n - u_{n/2}\|_2$	Ratio	$\log_2$(Ratio)
32			
64	0.025161873		
128	0.019001844	1.324180566	0.405099862
256	0.013886876	1.368331061	0.452417325
512	0.009941277	1.396890613	0.482219051
1024	0.006618258	1.50209863	0.586979545
2048	0.004422908	1.496358934	0.581456278

(b) First Order Godunov

n	$\|u_n - u_{n/2}\|_2$	Ratio	$\log_2$(Ratio)
32			
64	0.018546753		
128	0.016457235	1.126966489	0.172444617
256	0.014558409	1.130428142	0.176869287
512	0.012359751	1.177888577	0.236203073
1024	0.010409579	1.18734397	0.24773794
2048	0.008807568	1.181890292	0.241096125

the problems and the presence of flux-limiters. That said, the HR scheme uniformly outperformed the first order scheme both qualitatively and quantitavely. The same cannot be said for the "corner-correction", but that correction did yield qualitative improvements.

For future work, the we could achieve higher former order of convergence with Weighted Essentially Nonoscillatory (WENO) schemes. In fact, we implemented a fifth order scheme for the uniform advection scheme, but did not show the results here. For a review of these schemes in both the Finite Volume as well as Finite Difference framework see the review paper [3]. The application of such schemes to the SWE is described in [5].

Finally, for a complete analysis of the nonlinear Geostrophic Adjustment problem using these same schemes, please see [1].

Appendix

Roe Averaging for Shallow Water Equations

For 1D, the Roe averaging is given in [4, 2]. For 2 dimensions, it is relatively easy to show that a similar roe averaging operator works. In particular, for $\hat{u}$ and $\hat{v}$, use the weighted averaging defined as follows:

$$\hat{u} = \frac{\sqrt{h_l}u_l + \sqrt{h_r}u_r}{\sqrt{h_l} + \sqrt{h_r}}.$$

While for $\bar{h}$ use a simple arithmatic average.

Then the flux matrices in the x and y directions are respectively

$$\hat{A} = \begin{pmatrix} 0 & 1 & 0 \\ -\hat{u}^2 + g\bar{h} & 2\hat{u} & 0 \\ \hat{u}\hat{v} & \hat{v} & \hat{u} \end{pmatrix}$$

and

$$\hat{B} = \begin{pmatrix} 0 & 1 & 0 \\ -\hat{u}\hat{v} & \hat{v} & \hat{u} \\ -\hat{v}^2 + g\bar{h} & 0 & 2\hat{v} \end{pmatrix}.$$

These results are derived using by setting $z_i = q_i/\sqrt{h}$ and proceding as in the book.

These matrices are just the Jacobian matrices of the fluxes with the Roe-averaged quantities inserted.

References

[1] AC Kuo and LM Polvani. Time-dependent fully nonlinear geostrophic adjustment. *Journal of physical oceanography*, (Stoker 1958):1614–1634, 1997.

[2] Randall LeVeque. Finite volume methods for hyperbolic problems, 2002.

[3] Chi-Wang Shu. High Order Weighted Essentially Nonoscillatory Schemes for Convection Dominated Problems. *SIAM Review*, 51(1):82–126, February 2009.

[4] Geoffrey K Vallis. *Atmospheric and oceanic fluid dynamics: fundamentals and large-scale circulation*. Cambridge University Press, Cambridge, 2006.

[5] Yulong Xing and Chi-Wang Shu. High order finite difference WENO schemes with the exact conservation property for the shallow water equations. *Journal of Computational Physics*, 208(1):206–227, September 2005.